Characterization of Grooves in Scratch Resistance Testing

Witold Brostow,[1] **Wunpen Chonkaew,**[1] **Reza Mirshams,**[2] **Ashish Srivastava**[3]
[1] *Laboratory of Advanced Polymers & Optimized Materials (LAPOM), Department of Materials Science and Engineering, College of Engineering, University of North Texas, Denton, Texas 76201-5310*

[2] *Department of Engineering Technology, College of Engineering, University of North Texas, Denton, Texas 76201-5310*

[3] *Department of Materials Science and Engineering, College of Engineering, University of North Texas, Denton, Texas 76201-5310*

For a number of polymers with different chemical structures and different properties we have determined scratch resistance and sliding wear (15 scratches along the same groove). We have measured cross section areas after scratching, namely the groove and side top-ridge areas. Nanohardness after scratching was determined using nanoindentation testing both inside and outside the scratching and sliding wear grooves. Three modes of sliding wear are seen: plowing, cutting with debris formation, and densification. The dominating mode depends on the material and is reflected in nanohardness. In polycarbonate (PC) the nanohardness inside and outside the groove are practically the same; the indenter just plows the material aside without debris formation or densification. Thus, the old measure of wear as the weight of the debris formed is not usable for PC; grooves are present but there is no loosened material. By contrast, in brittle materials such as polystyrene there is debris formation and nanohardness inside the groove decreases after 15 scratching runs. A third type of behavior is seen in polyethylene and polypropylene, namely densification caused by scratching; as a result, nanohardness inside the groove increases after 15 passes of the indenter. **POLYM. ENG. SCI., 48:2060–2065, 2008.**

INTRODUCTION

Determination of scratch resistance is one of the most important aspects of tribology of materials, together with friction and wear. As discussed in the literature [1–3], polymer tribology is much more difficult than that of metals. Because of the gradual replacement of metal parts by polymeric ones, the need to understand tribological behavior of polymers is increasing.

There are two main lines of work here: one is improving the tribological properties of specific polymers. Blending with a fluoropolymer [4], addition of an inorganic or carbon nanotubes filler [5, 6] and γ-irradiating the surface [7] have been used to migitage wear and to lower friction. Another approach consists in improved understanding of wear mechanisms in polymers.

Many mechanisms have been proposed to explain wear; however, this was mostly done for metals. The interesting mechanisms are the formation of plastic deformation and strain hardening during the sliding contact.

Yoshida et al. discuss densification of glasses caused by indentation [8]. Now consider the finding of Bhushan et al. [9] that microhardness measurements of worn metal samples show a 10–80% increase of hardness in the worn layer. Although behavior of the metals is different from that of polymers since the latter are viscoelastic, a possible connection between the characteristics of groove profiles we have obtained with hardness determination seemed worth pursuing.

In this work, we are interested in studying possible mechanisms of tribological events occurring in polymers. We have performed the sliding wear determination on several kinds of polymers, investigated the profiles of tracks and determined the hardness inside the wear tracks compared with that of polymers without wear.

HARDNESS MEASUREMENTS

In order to determine the hardness, we have used depth sensing indentation (nano indentation). The indentation

Correspondence to: Witold Brostow; e-mail: brostow@unt.edu
Contract grant sponsor: Robert A. Welch Foundation, Houston; contract grant number: B-1203; contract grant sponsor: Royal Thai Fellowship, Bangkok.
DOI 10.1002/pen.21085
Published online in Wiley InterScience (www.interscience.wiley.com).

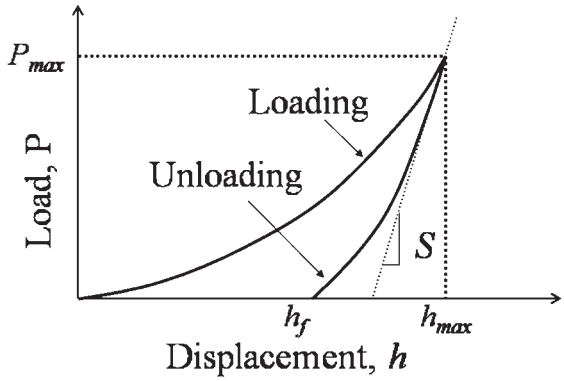

FIG. 1. Typical load versus displacement curve.

response allows hardness and elastic modulus to be evaluated. As the indenter is driven into the material, an impression conforming to the shape of the indenter to some contact depth h_c appears. As the indenter is withdrawn, only the elastic portion of the displacement is recovered. A typical force displacement curve showing the loading and unloading step is shown in Fig. 1. The important quantities are the peak load P_{max}, displacement h_{max}, the residual depth after unloading h_f (determined by curve fitting), and the slope of the initial portion of the unloading curve known as the elastic stiffness of the contact $S = dP/dh$. The local hardness H can be calculated as [10]:

$$H = P/A \tag{1}$$

where P is the load applied to the test surface and A is the projected contact area at that load.

One of the primary distinctions between depth sensing indentation and conventional microhardness testing is the manner in which the contact area is established from an analysis of the load-displacement data – rather than by imaging of the indentation after the load is removed and measuring the diagonal lengths [11].

The most widely used method for calculating the contact area has been developed by Oliver and Pharr [12, 13]. It has been developed for elastic materials only—a fact that needs to be remembered applying their approach to any other materials. One fits depth versus load unloading data to a power law function:

$$P = B(h - h_f)^m \tag{2}$$

where h is the resulting penetration while B and m are empirically determined fitting parameters. The unloading stiffness S is then obtained by differentiating *Eq. 2* and evaluating at the maximum penetration depth h_{max}, so that

$$S = Bm(h - h_f)^{m-1/h_{max}} \tag{3}$$

The next step in the procedure is the determination of the contact depth of the material with the indenter h_c, namely

$$h_c = h - \varepsilon P/S \tag{4}$$

where ε is equal to 0.75 for Berkovich type indenters.

Finally, the projected contact area is derived as a function of the contact depth h_c

$$A = f(h_c) \tag{5}$$

EXPERIMENTAL

We have selected low density polyethylene (LDPE), polypropylene (PP), polycarbonate (PC), polystyrene (PS), and acrylonitrile/butadiene/styrene (ABS) for this study because of differences in their mechanical properties and their variety of applications. LDPE is a commodity thermoplastic, supplied by Huntsman. PC and ABS are engineering thermoplastics, supplied by the Dow Chemical. PS is a brittle thermoplastic [14] purchased from Aldrich Chemicals. Polypropylene (PP) was supplied by Phillips.

To prepare groves on the polymer surfaces, we have used a Micro Scratch Tester (MST) from CSEM Instruments in both a single scratch and multiscratch modes. The procedure and instrument used were described in detail before [2, 3, 15]. A conical indenter with a diamond tip with the radius of 200 μm and the conical angle of 120° was drawn over the polymer surfaces, the load applied was 15.0 N. The scratch speed was 5.0 mm/min. The scratch length was 5.0 mm. To determine sliding wear, 15 scratches along the same original groove were performed using the same parameters as in a single scratch resistance determination.

Samples with grooves obtained from sliding wear determination were coated with gold. The sample surfaces were then studied using FEI Nova 200 Dual Beam FIB/FEGSEM apparatus.

We have performed the nanoindentation testing using MTS NanoIndenter XP. A Berkovich (three-side pyramidal) diamond indenter was used throughout the experiments in order to determine the nanohardness of specimens both inside and outside the wear tracks. The method used was XP basic hardness, modulus, load control. Allowable drift rate is 0.050 nm/s. Indentations were load-controlled to 1 gf maximum load. This load was found as an optimal one after conducting a range of experiments to reach a residual depth of approximately 2000 nm on all of the above materials. The time to load was 20 s. Peak hold time was 45 s to account for the visco-elastic nature of polymeric materials. The percentage to unload was 90%. At least three tests were performed on each of the polymeric samples at various locations in the specific region, namely inside the groove or outside the groove of a given sample.

Surface profiles across the groove made on each polymer were determined using a profilometer, model Surtronic 3+ from Rank Tailor Hobson Each such profile was determined perpendicularly to the side of the groove and through the center of the groove. The areas of the groove

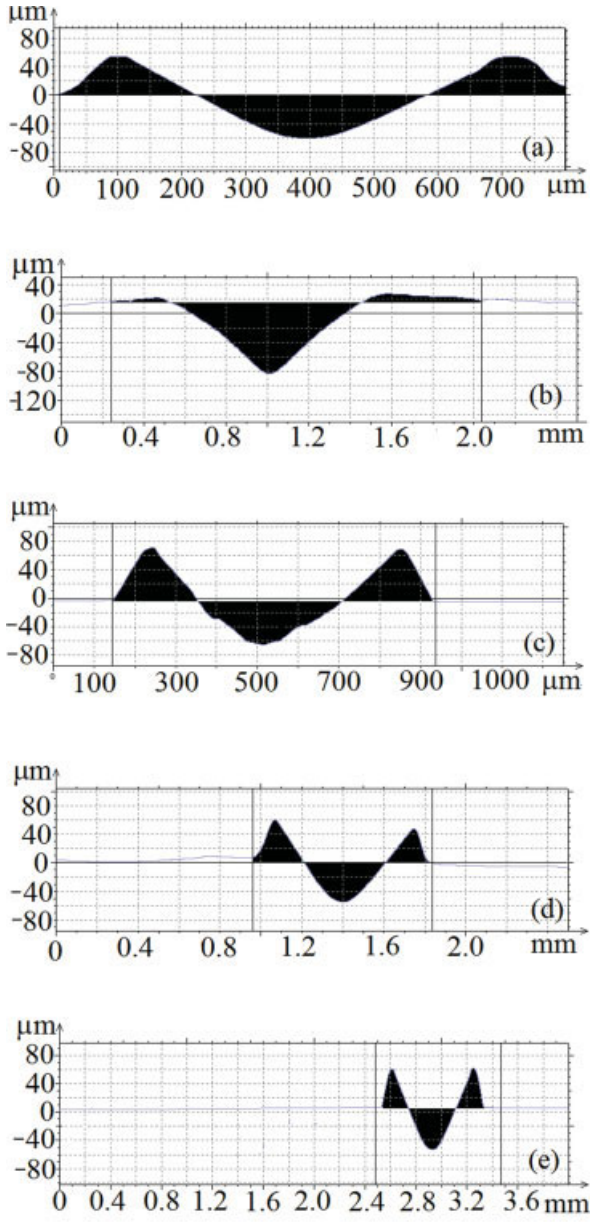

FIG. 2. A Profile of a scratch trace on a surface of (a) ABS (b) LDPE (c) PS (d) PP and (e) PC after applying a load of 15.0 N along the same groove for 15 times. Each profile is perpendicular to the side and goes through the center of the groove. [Color figure can be viewed in the online issue, which is available at www.interscience.wiley.com.]

were thus determined. We distinguish here between the area below the original planar surface of groove A_i and the area of the ridges A_o. The subscripts stand respectively for inside and outside. We have determined earlier groove profiles after a single scratch run [16]. Thus, we shall also see how multiple scratching (15 times in our sliding wear determination) affects the grooves.

PROFILES OF WEAR TRACKS

The surface profiles across the groove formed after applying a load of 15.0 N along the same groove for 15 times are shown in Fig. 2. For PP, PC, PS, and ABS, a passage of the indenter results in the formation of a groove and also in the formation of top-ridges along both sides of the groove. This ridge formation implies a plastic deformation according to the original classification. It has been proposed by Dinelli et al. [17] that the ridge-formation deformation in polymer occurs via molecular displacement and conformational changes rather than by bond breaking. However, for LDPE we have found that there is no well defined ridge-formation. To demonstrate the phenomenon clearly, we have plotted the bar graph showing the comparison of the area below the original planar surface of groove A_i and the area of the ridges A_o above that surface for each polymer (see Fig. 3).

We see in Fig. 3 that—except for PE—the area of the ridges A_o and the area of the groove are quite similar, especially in the case of PC. In the PC case the difference between these two areas is less than 1%. As seen below in a SEM micrograph (see Fig. 4), the surface of PC after applying a load of 15.0 N along the same groove for 15 times is pretty smooth and the ridges formed along the side of the groove are clearly observed. Thus, apparently that wear mechanism for PC involves mainly the material deformation and pile-up as top ridges. The indenter has plowed the materials along the sides when passing through without removing the material.

As mentioned, the surfaces inside the grooves of PP, PC, ABS, PS, and LDPE using SEM as shown in Fig. 4. The surface of ABS after applying a load of 15.0 N along the same groove for 15 times is fairly smooth. Ridges together with traces of cutting pieces (ribbon-like) formed along the side of the groove are clearly observed.

As observed by Durand et al. [18], the groove surface of PS is wavelike along the sliding direction and shows cracks, a consequence of PS brittleness pointed out before [14] and now confirmed [19]. The wedging formation has

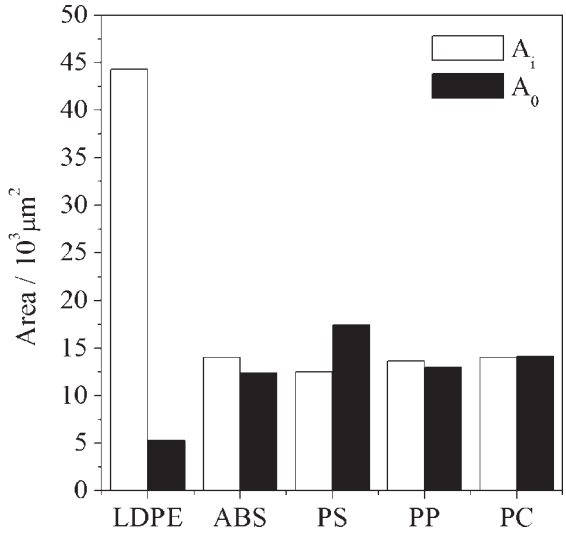

FIG. 3. The comparison of the area of groove A_i below the original planar surface and the area of the side top ridges A_o.

DOI 10.1002/pen

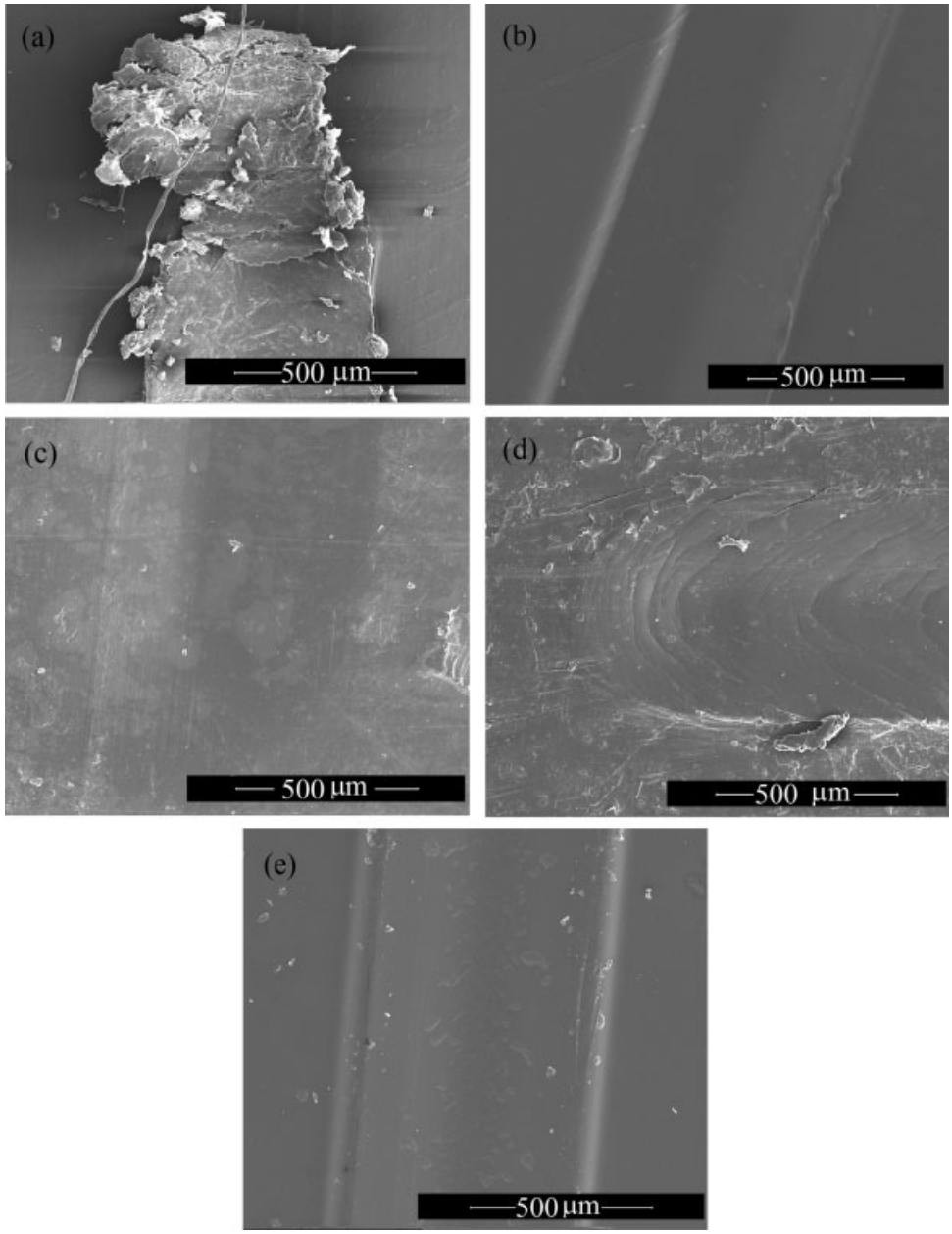

FIG. 4. SEM micrograph at magnification of ×100 of (a) PS (b) ABS (c) LDPE (d) PP (e) PC after applying a load of 15.0 N along the same groove for 15 times.

also been observed at the end of the groove. Thus, the results from SEM together with those from Figs. 2 and 3 provide us with the mechanism of the wear in PS when the indenter slides through the surface. The material is not only displaced along the side of the plowed grooves but is also removed as small chips or develops a wedge on its fronts.

On the other hand, as we have seen from the light shadow trace in Fig. 4c, the surface of LDPE is smooth. There is no evidence of cutting, wedging and/or chip-formation. The ridge areas for LDPE so much smaller than the groove area can hardly come from material removal or wedge formation. Thus, the densification mode seems to be the most probable explanation of its mechanism, as suggested before as a hypothesis on the basis of single scratch testing [16]. The present results for sliding wear determined in 15 scratching runs confirm the earlier conclusion.

NANOHARDNESS

Given the above results, in order to investigate a possible densification occurring after wear, we have performed the nanohardness measurements for each polymer both in a single scan wear track and a 15th-scan wear track and compared with the hardness outside the groove. The results so obtained are shown in Fig. 5. Nanohardness

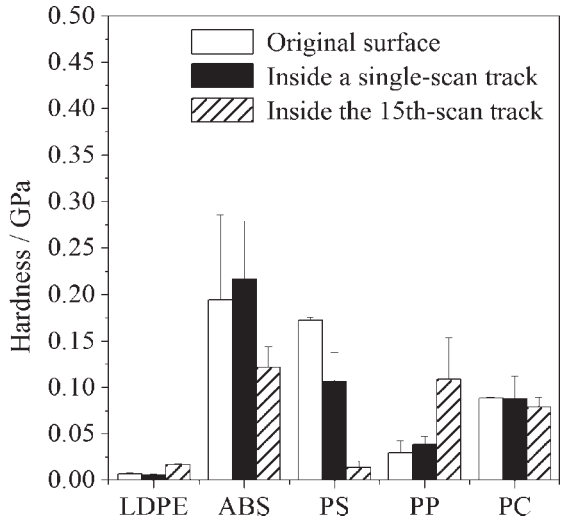

FIG. 5. Nanohardness of polymers inside and outside the groove.

inside the groove of all polymers after passing a single scan of the indenter is not much different from that of outside the groove. However, the differences between the two are much larger after 15 scans of the scratching indenter.

For LDPE and PP, nanohardness inside the groove increases after passing 15 scans of the indenter. The increase in hardness is a good evidence for the densification of the material by indentation.

For PS and ABS, nanohardness inside the groove decreases after passing 15 scans of the indenter. The possible explanation is that the failure of the surface have occurred after 15 scans of the indenter—as seen in the SEM micrograph (Fig. 4b).

As for PC, nanohardness inside the groove after passing 15 scans of indenter is similar to that outside the groove. This result supports our explanation above: for PC only material deformation and ridge formation occur. The indenter just plows the material aside without causing failure or densification. Thus, there is neither a decrease nor an increase of nanohardness.

We would like to recall that nanoindentation creep has been related to the glass transition [20]. The creep occurs differently above, below and around the glass transition.

GENERAL DISCUSSION

As discussed by Rabinowicz, the material removal from the surface via deformation during hard surface sliding on a soft surface, called abrasive wear, can occur by several deformation modes including plowing, wedge formation and cutting [1]. According to Myshkin et al. [21] in the case of polymeric materials there are two prominent modes of deformation. The first is the plowing mode in which a material is displaced sideways to form a top-ridge but no material is removed. The wear mechanism of PC belongs to this mode. The second is cutting in which the material displaced is removed as small debris pieces. Our results shown in Figs. 3 and 4 indicate that both phenomena take place in case of PS and ABS. The wedging and/or cutting process seems to occur together with the plowing process. The top-ridges can contain both material pushed to the side and some removed from the groove by wedging or cutting. Beyond these, we now have demonstrated a third mode of wear mechanism in sliding wear, namely densification, seen clearly in the case of LDPE and PP. Instead of top-ridge formation, the densification occurs when the material is deformed by the indenter.

It has been argued before that the depth after 15th scratch is a better measure of wear than the still used debris weight [22]. Our present results show that—at least in the case of polycarbonate—the old measure is useless since no debris is formed. We have shown before [23] that the penetration depth after 15th scratch is a function of $\tan\delta$ determined in dynamic mechanical analysis (DMA). A succinct description of results that DMA provides has been written by Menard [24]. Overall, a more detailed picture of the sliding wear now emerges. The experimental results for scratching and sliding wear can be confronted with molecular dynamics computer simulations of scratching non-crystals [25, 26].

ACKNOWLEDGMENTS

Oscar Olea is acknowledged for his help with SEM measurements. And last but not the least, we thank Prof. Yakov Soifer and the late Prof. Armen Verdyan for their help with the profilometer.

REFERENCES

1. E. Rabinowicz, *Friction and Wear of Material*, 2nd ed., Wiley, New York (1995).
2. W. Brostow, J.-L. Deborde, M. Jaklewicz, and P. Olszynski, *J. Mater. Ed.*, **25**, 119 (2003).
3. M.D. Bermúdez, W. Brostow, F.J. Carrión-Vilches, J.J. Cervantes, and D. Pietkiewicz, *Polymer*, **46**, 347 (2005).
4. W. Brostow, P.E. Cassidy, H.E. Hagg, M. Jaklewicz, and P.E. Montemartini, *Polymer*, **42**, 7971 (2001).
5. M. Ochi, R. Takahashi, and A. Terauchi, *Polymer*, **42**, 5151 (2001).
6. W. Brostow, B.P. Gorman, and O. Olea-Mejia, *Mater. Lett.*, **61**, 1333 (2007).
7. W. Brostow, M. Keselman, I. Mironi-Harpaz, M. Narkis, and R. Peirce, *Polymer*, **46**, 5058 (2005).
8. S. Yoshida, J.C. Sangleboef, and T. Rouxel, *J. Mater. Res.*, **20**, 3404 (2005).
9. B. Bhushan, R.E. Davis, and H.R. Kolar, *Thin Solid Films*, **123**, 113 (1985).
10. The manual for The Nano Indenter® XP from MTS System Corporation.
11. M.F. Doerner and W.D. Nix, *J. Mater. Res.*, **1**, 601 (1986).
12. W.C. Oliver and G.M. Pharr, *J. Mater. Res.*, **7**, 1564 (1992).

 DOI 10.1002/pen

13. W.C. Oliver and G.M. Pharr, *J. Mater. Res.*, **19**, 3 (2004).
14. W. Brostow, H.E. Hagg Lobland, and M. Narkis, *J. Mater. Res.*, **21**, 2422 (2006).
15. W. Brostow, B. Bujard, P.E. Cassidy, H.E. Hagg, and P. Montemartini, *Mater. Res. Innovat.*, **6**, 7 (2001).
16. W. Brostow, W. Chonkaew, L. Rapoport, Y. Soifer, and A. Verdyan, *J. Mater. Res.*, **22**, 2483 (2007).
17. F. Dinelli, G.J. Leggett, and P.H. Shipway, *Nanotechnology*, **16**, 675 (2005).
18. J.M. Durand, M. Vardavoulias, and M. Jeandin, *Wear*, **181–183**, 833 (1995).
19. W. Brostow and H.E. Hagg Lobland, *in the same issue*.
20. B.D. Beake, G.A. Bell, W. Brostow, and W. Chonkaew, *Polym. Int.*, **56**, 773 (2007).
21. N.K. Myshkin, M.I. Petrokovets, and A.V. Kovalev, *Tribol. Inter.*, **38**, 910 (2005).
22. W. Brostow, G. Damarla, J. Howe, and D. Pietkiewicz, *e-Polymers*, **25**, 1 (2004).
23. W. Brostow, W. Chonkaew, and K.P. Menard, *Mater. Res. Innovat.*, **10**, 389 (2006).
24. K.P. Menard, Ch. 8 in *Performance of Plastics*, ed., W. Brostow, Hanser, Munich (2000).
25. W. Brostow, J.A. Hinze, and R. Simões, *J. Mater. Res.,* **19**, 851 (2004).
26. W. Brostow and R. Simões, *J. Mater. Ed.* **27**, 19 (2005).